density and over a wide range of temperature. Application of the correlation requires the limiting low pressure value for the desired gas, obtained by measurement or calculation by the Chapman-Enskog theory.

ACKNOWLEDGMENT

The authors wish to thank National Science Foundation for the support of this work and Phillips Petroleum Company for generous supply of hydrocarbons.

NOTATION

A = echo amplitude
b, c, d = coefficients in polynomial
C = concentration of component
D = self-diffusion coefficient (sq.cm./sec.)
G = magnetic field gradient
k = constant; Boltzmann's constant
M = molecular weight
P = pressure
R = gas law constant
r = mean square net distance a molecule moves in time t
T_2 = spin-spin relaxation time
t = time delay of echo following exciting pulse
γ = nuclear gyromagnetic ratio
ρ = density, (g./cc.)
ϵ/k, σ = Lennard-Jones parameters, °K. and Å.
$\Omega^{(1,1)*}$ = collision integral, a function of kT/ϵ

Subscripts

c = critical
o = low density limit
r = reduced

LITERATURE CITED

1. Bearman, R. J., *J. Chem. Phys.*, **32**, 1308 (1960).
2. Carr, H. Y., and E. M. Purcell, *Phys. Rev.*, **94**, 630 (1954).
3. Dawson, R., Ph.D. thesis, Rice Univ., Houston, Tex. (1966). Available from University Microfilm, Ann Arbor, Michigan.
4. Douglass, D. C., and D. W. McCall, *J. Phys. Chem.*, **62**, 1102 (1958).
5. ———, and E. W. Anderson, *J Chem. Phys.*, **34**, 152 (1961).
6. Durbin, L., and R. Kobayashi, *ibid.*, **37**, 1643 (1962).
7. Hahn, E. L., *Phys. Rev.*, **80**, 580 (1950).
8. Hartland, A., and M. Lipsicas, *ibid.*, **133A**, 665 (1964).
9. Hirschfelder, J. O., C. F. Curtiss, and R. B. Bird, "Molecular Theory of Gases and Liquids," Wiley, New York (1954).
10. Lispicas, M., *J. Chem. Phys.*, **36**, 1235 (1962).
11. Mason, E. A., and W. E. Rice, *ibid.*, **22**, 843 (1954).
12. Mifflin, T. R., and C. O. Bennett, *ibid.*, **29**, 975 (1958).
13. Mueller, C. R., and R. W. Cahill, *ibid.*, **40**, 651 (1964).
14. Naghizadeh, J., and S. A. Rice, *ibid.*, **36**, 2710 (1962).
15. O'Hern, H. A., and J. J. Martin, *Ind. Eng. Chem.*, **47**, 2081 (1955).
16. Oosting, P. H., Dissertation, Univ. Amsterdam, Netherlands (1968).
17. Slattery, J. C., and R. B. Bird, *AIChE J.*, **4**, 137 (1958).
18. Trappeniers, N. J., and P. H. Oosting, *Phys. Letters*, **23**, 445 (1966).
19. Vennix, A. J., and Riki Kobayashi, *AIChE J.*, **15**, No. 6, 926 (Nov., 1969).
20. Winn, E. B., *Phys. Rev.*, **80**, 1024 (1950).

Manuscript received July 26, 1968; revision received December 23, 1968; paper accepted December 30, 1968.

Small Surface Waves and Gas Absorption

G. F. DICK, JR., and J. M. MARCHELLO
University of Maryland, College Park, Maryland

Surface renewal models based on wave induced drift currents are proposed to explain gas absorption data in deep tanks. A model assuming plug surface flow was found to best represent the available data for the absorption of carbon dioxide, oxygen, propylene, and helium into water. Velocities obtained by fitting the mass transfer data agree with experimental velocities obtained from dye studies.

Small waves or ripples have been observed to have a pronounced effect on mass transfer across an air-water interface (*1*, *6*). Goren and Mani (*4*) studied the effect of standing waves of controlled amplitude and frequency on mass transfer through thin, horizontal, liquid layers. They also conducted dye studies of the drift currents produced by the waves. The objective of this investigation was to study drift motions induced by progressive waves and to develop an applicable absorption model.

SURFACE RENEWAL MODELS

Absorption in water is described by the general equations of change for species conservation. The velocity components may, in principle, be obtained from wave hydrodynamics. Classical first-order wave theory predicts smooth closed particle paths which are ellipses for deep water progressive waves (*7*). When second-order terms are included, closed particle paths are no longer predicted (*5*), and there is a net drift velocity.

Stokes (*8*) proposed a simple expression for the second-order mean velocity in the direction of wave propagation for inviscid fluids. More recently, Longuet-Higgins (*5*) has developed an expression for the wave drift velocity for viscid fluids. Comparisons of the Longuet-Higgins and Stokes theories with experimental data have been inconclusive (*9*), but it appears that the Stokes expression is most applicable for deep water waves ($kd > 1$), while the Longuet-Higgins solution best describes shallow water transport.

In the development of the surface renewal models, it is assumed that the water flows away from the generator along the surface. The surface drift flow is strong but shallow and is present over less than one fifth of the total

---

G. F. Dick, Jr., is with Esso Research and Engineering Company, Baytown, Texas.

depth. It is further assumed that the water at the gas-liquid interface is saturated and that the gas diffuses molecularly into the rapidly moving surface waters. At the end of the tank, the water submerges and becomes thoroughly mixed so that all of the subsurface water has the bulk concentration.

For sparingly soluble gases, the bulk concentration changes slowly with time, and pseudo steady state diffusion into the surface layer is assumed. Also, for two-dimensional small amplitude waves with a laminar drift velocity u, the resulting equation for diffusion of absorbed gases in water is

$$u \frac{\partial C}{\partial x} = D \frac{\partial^2 C}{\partial z^2} \qquad (1)$$

The boundary conditions are

$$C(0, z) = C_0 \qquad (2)$$

$$C(x, 0) = C_i \qquad (3)$$

$$C(x, \infty) \neq \infty \qquad (4)$$

The first boundary condition requires that the water coming to the surface at the generator be at the bulk concentration C_0. As soon as it reaches the surface and is exposed to the pure gas, the water becomes saturated as shown in Equation (3). In the interior of the fluid, the concentration is finite.

The Stokes expression for the drift velocity profile for infinite depth of liquid is

$$u = a^2 \sigma k e^{-2kz} \qquad (5)$$

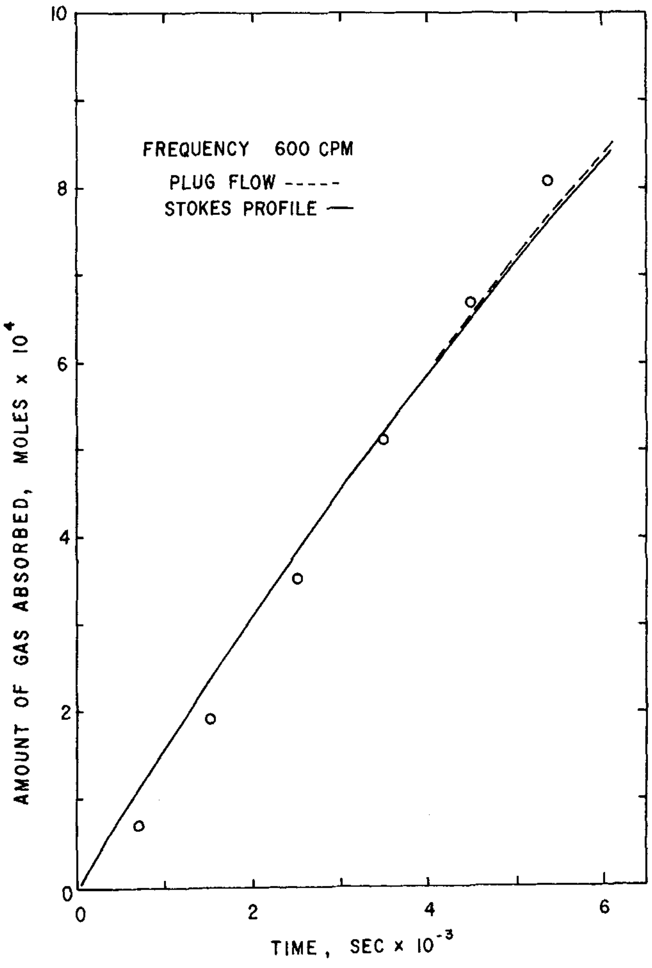

Fig. 1. Comparison of gas absorption models with oxygen data.

The solution to Equations (1) and (5) with Equations (2), (3), and (4) was obtained by using the method of Laplace transforms (3). The solution in terms of the dimensionless concentration Γ is

$$\Gamma(x, z) = 1 - 2 \sum_{n=1}^{\infty} \frac{e^{-\frac{Dk\lambda_n^2 x}{a^2\sigma}} \qquad J_0(\lambda_n e^{-kz})}{\lambda_n J_1(\lambda_n)} \qquad (6)$$

To complete the model, an expression for Δn, the total moles of gas absorbed in the water at any time, must be obtained. The model assumes a pseudo steady state for relatively short periods of times in the order of several minutes. Time changes of a larger scale are brought in by use of the material balance

$$\frac{d\,\Delta n}{d\theta} = -DW\left(C_i - \frac{\Delta n}{V}\right) \int_0^L \left(\frac{\partial \Gamma}{\partial z}\right)_{z=0} dx \qquad (7)$$

Differentiating Equation (6) and substituting it in Equation (7), we get an integro-differential equation, the solution of which is

$$\Delta n = C_i V \left[1 - e^{-\frac{2\theta}{Ld} \sum_{n=1}^{\infty} \frac{a^2\sigma}{\lambda_n^2} \left\{ 1 - e^{-\frac{Dk\lambda_n^2 L}{a^2\sigma}} \right\}} \right] \qquad (8)$$

assuming that initially there is no dissolved gas in the water.

In like manner, Equation (1) was solved by assuming that the velocity was constant or in plug flow (3). The resulting expression for the amount absorbed is

$$\Delta n = C_i V \left[1 - e^{-\frac{2\theta}{d}\sqrt{\frac{\overline{U}D}{L\pi}}} \right] \qquad (9)$$

In this instance, Equation (4) was replaced with

$$C(x, \infty) = C_0 \qquad (10)$$

Finally, an expression similar to Equation (9) was obtained by using a constant mass transfer coefficient defined by

$$N = k_L (C_i - C_0) \qquad (11)$$

and an unsteady state material balance similar to Equation (7). The mass transfer coefficient result and the plug flow expression, Equation (9), are identical (3) when

$$k_L = 2\sqrt{\frac{\overline{U}D}{\pi L}} \qquad (12)$$

Thus, there is no significant difference between the plug flow surface renewal model and the use of a mass transfer coefficient for pseudo steady state absorption. The difference between Equations (8) and (9) is due to the use of the Stokes drift velocity. Since the eddy flux $-\overline{w'C'}$ was omitted from Equation (1), the D used in Equations (1) through (12) is an effective diffusivity.

The models presented above were fitted to the data of Muenz and Marchello (6) for the absorption of pure helium, oxygen, propylene, and carbon dioxide. They used a small enclosed ripple tank with the wave generator located in the center of the tank. The amount of gas absorbed was measured as a function of time in a series of unsteady state runs.

The amplitude in Equation (8) was used as a fitting parameter for the gas absorption data. Wavelength data were taken from reference *6*. A computer program was written to determine the least-squares fit of the data for each run (*3*), and the resulting amplitudes were expressed in terms of the surface velocity

$$U_s = a^2 \sigma k \tag{13}$$

In a similar manner, Equation (9) was fitted to the data by using the plug flow velocity as a fitting parameter. The resulting velocities and percent standard deviations are given in Table 1. The plug flow model gave a slightly better fit than the Stokes model. A typical result is shown in Figure 1.

DRIFT AND SURFACE VELOCITIES

A series of experiments were conducted to study the water drift circulation patterns in order to substantiate the flow patterns assumed for the surface renewal models. The equipment used by Muenz was employed here. The ripple tank (*1, 3, 6*) was constructed of ¾-in. Plexiglass. It was 50 cm. long, 16 cm. wide, and 10 cm. deep. The wave generator was located in the center. The water depth for all runs considered here was 5 cm. Talc was used to observe and measure the surface flows, and methylene blue dye was injected at various locations in the water to study the subsurface flows.

Several transparent scales were mounted on the tank and used to determine the distance traveled by the talc or dye. Time of travel was measured with a stopwatch. During these experiments the tank was open. Before any measurements were made, the generator was run for 45 min. to stabilize the flow patterns.

Individual flow patterns were determined by continuously injecting dye at a point. The flow velocity was measured by injecting a small amount of dye at a point, by using a hand syringe, and then by timing the travel with a stopwatch. All measurements were repeated numerous times, so that the reported results consist of average values.

Drift velocities for 400, 600, and 800 cycles/min. and flow patterns for 600 cycles/min. are presented in Table 2 and Figure 2, respectively. In the top view of Figure 2, the tank front is the lower portion. In addition to changes in velocity with frequency, definite variations in the surface pattern were observed. The patterns were basically circular, with the main source of flow originating at the side of the generator at 400 cycles/min. As the frequency increased, the flow source moved toward the center of the generator, and the water then returned along the sides of the tank.

Subsurface patterns remain the same for all three frequencies. On the right side, water originating near the bottom of the generator surfaced at 5 or 6 cm. out, continued to move outward to about 18 cm., submerged, and returned along the bottom. The subsurface patterns on the left side were similar, except that the water surfaced closer to the generator.

DISCUSSION

The velocities in Table 1 were obtained by fitting each of the absorption runs of Muenz (*6*) to Equations (8) and (9). Comparison of the data in Tables 1 and 2 indicates that the velocities obtained by fitting the mass transfer data are lower than the observed velocities. There are three possible explanations for this. First, the observed velocities near the ends of the tank were much slower than those in the first two thirds of the distance from the generator. An average velocity over the entire length of the tank would lower the observed speeds. Also, differences in effective mass transfer areas could account for the velocity discrepancies. During the drift pattern studies, stagnant areas were observed in corners, and there was some return flow along the surface at the sides of the tank. Since the models assumed unidirectional, uniform flow to the end of the tank before submergence, the velocity required for the models would be less than that which was measured for the experimental surface area. The third explanation may be due to the eddy flux term for transfer across the free surface (*6*).

Mass transfer coefficients were calculated from the data of Table 1 and Equation (12). They ranged from 0.009 to 0.045 cm./sec. and were directly proportional to both the frequency and molecular diffusivity. Davies, Kilner, and Ratcliff (*9*) found similar dependencies for

Table 1. Results of Velocity Fits for Surface Renewal Models

		Stokes velocity profile		Plug flow velocity	
Absorbing gas	Frequency, cycles/min.	Surface velocity, cm./min.	Percent std. deviation	Plug flow velocity, cm./min.	Percent std. deviation
Oxygen	400	3.86	8.50	3.08	8.37
	600	5.16	14.82	3.82	14.70
	600	6.59	8.84	5.32	8.80
	800	7.37	9.99	5.35	9.92
Propylene	400	2.17	6.82	1.83	6.54
	600	3.52	6.72	2.63	6.25
	800	5.33	8.52	4.05	8.51
	800	4.15	5.22	2.97	5.06
Helium	400	10.61	18.56	8.77	18.56
	400	8.70	13.58	7.13	13.58
	600	13.35	8.74	10.35	8.85
	600	12.46	17.31	8.89	17.19
Carbon dioxide	400	11.42	1.78	9.92	1.60
	600	12.64	0.98	10.36	0.83
	600	12.64	1.23	10.58	1.15
	800	15.50	1.01	12.38	0.84

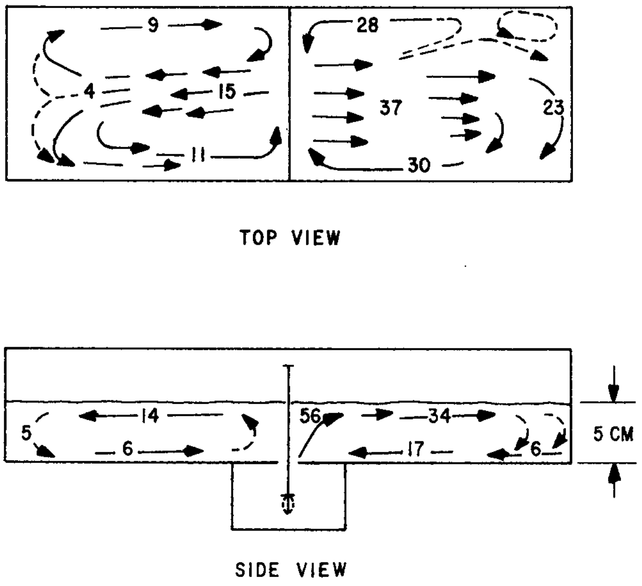

Fig. 2. Water drift patterns and velocities at 600 cycles/min.

Table 2. Surface and Subsurface Drift Velocities and Wave Frequencies for Gas Absorption Tank

Surface velocities (cm./min.)

Frequency, cycles/min.	Left side			Right side		
	Front return	Center	Back return	Front return	Center	Back return
400	5	7	6	16	25	25
600	11	15	9	30	37	28
800	12	25	8	42	72	43

Subsurface velocities (cm./min.)

Frequency, cycles/min.	Left side			Right side	
	Average surface velocity	Average bottom velocity	Surfacing velocity	Average surface velocity	Average bottom velocity
400	7	4	42	14	5
600	14	6	56	34	17
800	28	18	110	59	28*

* Average velocity of water returning along sides of tank.

absorption into water in a stirred tank. However, their coefficients differ from those obtained here by a factor of about 100, which is probably the result of greater mixing and turbulence.

Velocity depths and film thicknesses were calculated from the mass transfer coefficients (3). The velocity depth δ_v is that depth at which the depth average modified Stokes velocity is equal to the plug flow velocity:

$$\overline{U} = \frac{1}{\delta_v}\int_0^{\delta_v} U_s e^{-2kz}\, dz \qquad (14)$$

There is an inverse dependence of both the film thickness and velocity depth on the frequency and hence the drift velocity, but 0.10 cm. is representative for both film thicknesses and velocity depths. This represents the main justification for the success of the plug flow model. The absorbing gas penetrated only a small distance into the water, and the absorption was due primarily to the drift currents. The velocity that the gases saw was essentially the surface velocity. A profile such as that proposed by Stokes extends over about 1 cm. of depth for the conditions present in this investigation, but, because of the small penetration of the gas, a shallower, simpler velocity expression is sufficient.

The mass transfer coefficients for helium, oxygen, and propylene were found to correlate in terms of

$$N_{Sh} = 0.588\ (N_{Re})^{0.455} \qquad (15)$$

with the film thicknesses and velocity depths not dependent on the absorbing gas. The exponent of 0.455 in Equation (15) reflects the proportionality of the fitted velocities to frequency and the fact that the mass transfer coefficients were calculated from Equation (12). As previously observed (6), the carbon dioxide did not correlate with the data for the other gases.

In summary, drift currents were found to be primarily responsible for the transfer of gas into the water. The plug flow surface renewal model is favored because of its mathematical simplicity. The velocities resulting from fitting the data to the models were generally in agreement with experimental values obtained from dye studies, but they varied with Schmidt number. This weakness in the surface renewal models, which represents an inadequacy in explaining the hydrodynamics and mass transfer coupling, deserves attention in future investigations.

ACKNOWLEDGMENT

The authors wish to acknowledge the support of this research by the Division of Water Supply of the U.S. Department of Health, Education, and Welfare under U.S. Public Health Service Grant WP 00323.

NOTATION

a = wave amplitude = cm.
C = concentration of gas in water = moles/cc.
C' = concentration fluctuations = moles/cc.
C_i = concentration of gas in water at saturation = moles/cc.
C_0 = bulk concentration of gas in water = moles/cc.
D = molecular diffusivity of gas in water = sq.cm./sec.
d = depth of water = cm.
f = wave frequency = liter/sec.
k = $2\pi/\lambda$ = liter/cm.
k_L = mass transfer coefficient = cm./sec.
L = distance from wave generator to end of tank = cm.
N = molar absorption flux = moles/(sq.cm.)(sec.)
N_{Sh} = Sherwood number = $k_L d/D$
N_{Re} = Reynolds number = $fd^2 \rho/\mu$
$\overline{U}$ = plug flow velocity = cm./sec.
U_s = surface velocity = cm./sec.
u = laminar drift velocity = cm./sec.
V = volume of water = cc.
W = width of tank = cm.
w' = velocity fluctuation in vertical direction = cm./sec.
x = direction of wave propagation
z = depth from mean water level

Greek Letters

Γ = dimensionless concentration = $(C - C_0)/(C_i - C_0)$
Δn = amount of gas absorbed into water = moles
δ_v = velocity depth = cm.
λ = wavelength = cm.
λ_n = n^{th} root of $J_0\ (\lambda_n) = 0$
μ = viscosity = g./(cm.)(sec.)
ρ = density = g./cc.
σ = $2\pi f$ = liter/sec.
θ = time = sec.

LITERATURE CITED

1. Boyd, D. P., and J. M. Marchello, *Chem. Eng. Sci.*, **21**, 769 (1966).
2. Davies, J. T., A. A. Kilner, and G. A. Ratcliff, *ibid.*, **19**, 583 (1964).
3. Dick, G. F., Jr., Ph.D. thesis, Univ. Md., College Park (1969).
4. Goren, S. L., and R. V. S. Mani, *AIChE J.*, **14**, 57 (1968).
5. Longuet-Higgins, M. S., *Roy. Soc. London Phil. Trans.*, **245**, 536 (1953).
6. Muenz, Kurt, and J. M. Marchello, *AIChE J.*, **12**, 249 (1966).
7. Schwartz, R. J., and J. M. Marchello, *J. Geophysical Res.*, **173**, 5133 (1968).
8. Stokes, G. G., *Mathematical and Physical Papers*, **1**, 196 (1880).
9. Wiegel, R. L., "Oceanographical Engineering," p. 60, Prentice Hall, Englewood Cliffs, N. J. (1964).

Manuscript received October 8, 1968; revision received March 5, 1969; paper accepted March 14, 1969.